actuators

MDPI

Communication

Robust Stabilization of Underactuated TORA System Based on Disturbance Observer and Fixed-Time Sliding Mode Control Method

Qixuan Feng [1], Ancai Zhang [1,2,*], Xinghui Zhang [1,2], Guocheng Pang [1,2] and Zhi Liu [1,2]

[1] School of Automation and Electrical Engineering, Linyi University, Linyi 276000, China
[2] Key Laboratory of Complex Systems and Intelligent Computing in Universities of Shandong, Linyi 276000, China
* Correspondence: zhangancai@lyu.edu.cn; Tel.: +86-539-7258672

Abstract: A translational oscillator with a rotational actuator (TORA) is an underactuated nonlinear mechanical system with two degrees of freedom (DOF). This paper concerns the robust stabilization control problem for the system with multiple external disturbances. First, a disturbance observer is constructed based on the internal nonlinear dynamic behavior of the system. Second, a robust stabilization controller is designed by the estimated disturbances and the fixed-time sliding mode control method. The controller realizes the global robust stabilization control objective of the TORA system, and the stability of both disturbance observer and robust closed-loop control system are analyzed using the Lyapunov theorem. Finally, the effectiveness of the theoretical results are verified by numerical experiments.

Keywords: underactuated TORA systems; disturbance observer; fixed-time sliding mode; robust stabilization control

Citation: Feng, Q.; Zhang, A.; Zhang, X.; Pang, G.; Liu, Z. Robust Stabilization of Underactuated TORA System Based on Disturbance Observer and Fixed-Time Sliding Mode Control Method. *Actuators* **2022**, *11*, 271. https://doi.org/10.3390/act11100271

Academic Editor: Ioan Ursu

Received: 27 August 2022
Accepted: 20 September 2022
Published: 22 September 2022

1. Introduction

Underactuated systems are a class of mechanical systems with fewer control inputs than the system's degrees of freedom (DOF). These kinds of systems are widespread in everyday life. In order to study the motion control of underactuated systems, many underactuated models were established by scholars [1]. Among them, a translational oscillator with a rotational actuator (TORA) is a typical example. This model comes from a practical application problem. It describes the resonance-trapping phenomenon when a dual-spin spacecraft encounters resonance conditions during the spin process [2–5].

The TORA system has strong nonlinearity and has a nonholonomic constraint, and this system cannot be strictly feedback linearized. As a result, it is difficult to design the motion controller for the system. To solve the motion control problem for this system, researchers have developed many control methods in the past few years [6–11]. In [12], a recursive idea was used to construct the Lyapunov function, and a backstepping control law was designed. In [13], a passivity-based control law was developed by the cascade characteristics of the system from the energy point of view. In [14], a sliding mode surface was constructed, and a control law was designed to stabilize the system along the surface. On this basis, an adaptive sliding mode control method was presented in [15]. Moreover, a fuzzy Lyapunov synthesis method was used in [16] to design a feedback controller.

Although the abovementioned control methods are effective to stabilize the TORA, the design of the controller requires both the measurement information of velocity and the position of the system. In order to save costs, some attempts have been made in the controller design by using the position measurements only. For example, an equivalent input disturbance control method was developed in [17]. In addition, scholars also studied the stabilization control of the TORA when the saturation of control torque was concerned, and an anti-saturation feedback control law design method was presented [18,19] .

Although the presented method was very rigorous, the controller design was based on the nominal model of the TORA and did not consider the existence of external disturbance factors. As we all know, external disturbances are inevitable in the actual operating environment of a control system. So, it is necessary to study the robust stabilization control problem for the TORA system. In [20], a self-correction method was presented to infinitely approach the uncertainty disturbance in the system and a robust $H\infty$ controller was designed. In [21], a disturbance-observer-based methodology was utilized for the TORA system with unknown disturbances, and a sliding control law was presented to ensure the robust stabilization of the system. However, the disturbances considered were matched disturbance. That is, the considered disturbances exist in the control input channel. This design method is invalid when there are mismatched disturbances in the system.

At present, the design of a disturbance observer for a nonlinear system with unknown and/or unmeasured disturbances is a hotly discussed issue in the nonlinear control area. Some disturbance observer design methods were presented [22,23]. On the basis of previous research results, this paper further studies the global robust stabilization of the TORA system with multiple external disturbances including both matched and mismatched disturbances. The main research content of this paper has three parts. Firstly, we design a disturbance observer based on the internal nonlinear dynamics of the system. The multiple external disturbances can be quickly estimated by this observer. Secondly, a coordinate transformation is used to change the TORA to be a simple nonlinear system, and we design a robust stabilization controller for the new system by using the estimated disturbances and the fixed-time sliding mode control method. The controller ensures the global robust stabilization of the TORA to be achieved. Thirdly, the effectiveness of the proposed theoretical results are demonstrated via numerical experiments. This paper studies the robust control problem for the TORA system in a more practical operating environment. The developed controller has better practicability and adaptability. The research of this paper enriches the control theory system of an underactuated TORA system. It can be extended to the global robust stabilization of other underactuated mechanical systems.

2. Dynamic Motion Equations of TORA

As shown in Figure 1, the physical model of the TORA system consists of a cart and a small ball. The cart moves horizontally, and the ball oscillates in a two-dimensional vertical plane. One end of the cart is connected to a fixed vertical plane through a spring. There is an input force driving the ball to rotate. Due to the coupling relationship between the car and the ball, the motion of the ball can drive the car to move. It is clear that the TORA has two DOFs and has only one input torque. So, it is a typical 2-DOF underactuated mechanical system.

In Figure 1, M is the mass of the cart, m is the mass of the oscillating ball, k is the elastic coefficient of the spring, r is the radius of rotation, J is the torque, $x(t)$ is the displacement of the cart, $\theta(t)$ is the angle that the ball, and $\tau(t)$ is the driving force exerted on the ball. By a simple calculation, we respectively obtain the kinetic energy and potential energy of the TORA system as

$$T = \frac{1}{2}m[(\dot{x} + r\dot{\theta}cos\theta)^2 + (r\dot{\theta}sin\theta)^2] + \frac{1}{2}J\dot{\theta}^2,\ P = \frac{1}{2}kx^2.$$

We choose the Lagrangian function of the system to be $L = T - P$. By using the Euler–Lagrange modeling method [17], it is easy to obtain the following dynamic motion equations of the TORA system

$$\begin{bmatrix} M+m & mr\cos\theta \\ mr\cos\theta & mr^2+J \end{bmatrix}\begin{bmatrix} \ddot{x} \\ \ddot{\theta} \end{bmatrix} + \begin{bmatrix} -mr\dot{\theta}^2\sin\theta + kx \\ 0 \end{bmatrix} = \begin{bmatrix} d_1^* \\ \tau + d_2^* \end{bmatrix}, \quad (1)$$

where d_1^* and d_2^* are unknown external disturbances. For the nominal model of (1), it is easy to verify that the origin point $\left[x, \dot{x}, \theta, \dot{\theta}\right]^T = [0,0,0,0]^T$ is an open-loop equilibrium point of the system. The commonly discussed issue by researchers is to stabilize the TORA at the

equilibrium point. The main work of this paper is to eliminate the influence of external disturbances and to realize the robust stabilization control of the system at this point. We will describe how to use a disturbance observer and sliding mode control technology to design a robust controller τ below.

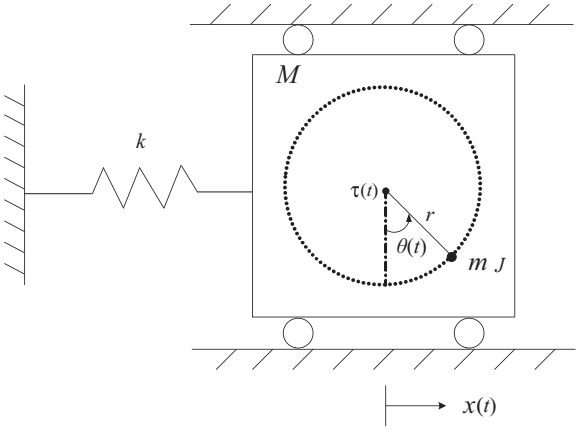

Figure 1. Physical model of the TORA system.

3. Design of a Disturbance Observer

In this section, a disturbance observer is constructed for (1) to estimate the unknown disturbances d_1^* and d_2^* . Here, it assumes that d_1^* and d_2^* are third-order differentiable and

$$\left\| \left[\begin{array}{cc} \frac{d^3 d_1^*}{dt^3} & \frac{d^3 d_2^*}{dt^3} \end{array} \right]^T \right\| \leq \zeta,$$

where ζ is a positive constant.

We change the system (1) into the following form

$$\left[\begin{array}{c} \ddot{x} \\ \ddot{\theta} \end{array} \right] = D^{-1}(\theta) \quad \left\{ \left[\begin{array}{c} 0 \\ \tau \end{array} \right] - \left[\begin{array}{c} -mr\dot{\theta}^2 \sin\theta + kx \\ 0 \end{array} \right] \right\} + \left[\begin{array}{c} d_1 \\ d_2 \end{array} \right], \tag{2}$$

where

$$D(\theta) = \left[\begin{array}{cc} M+m & mr\cos\theta \\ mr\cos\theta & mr^2 + J \end{array} \right], \quad \left[\begin{array}{c} d_1 \\ d_2 \end{array} \right] = D^{-1}(\theta) \left[\begin{array}{c} d_1^* \\ d_2^* \end{array} \right]. \tag{3}$$

Based on the expression of (2), a disturbance observer is designed to be

$$\begin{aligned} \left[\begin{array}{c} \dot{h}_{11} \\ \dot{h}_{21} \end{array} \right] &= -A\left(-D^{-1}(\theta) \left[\begin{array}{c} -mr\dot{\theta}^2 \sin\theta + kx \\ -\tau \end{array} \right] + \left[\begin{array}{c} \hat{d}_{10} \\ \hat{d}_{20} \end{array} \right] \right) + \left[\begin{array}{c} \hat{d}_{11} \\ \hat{d}_{21} \end{array} \right], \\ \left[\begin{array}{c} \hat{d}_{10} \\ \hat{d}_{20} \end{array} \right] &= \left[\begin{array}{c} h_{11} \\ h_{21} \end{array} \right] + A \left[\begin{array}{c} \dot{x} \\ \dot{\theta} \end{array} \right], \end{aligned} \tag{4}$$

$$\begin{aligned} \left[\begin{array}{c} \dot{h}_{12} \\ \dot{h}_{22} \end{array} \right] &= -B\left(-D^{-1}(\theta) \left[\begin{array}{c} -mr\dot{\theta}^2 \sin\theta + kx \\ -\tau \end{array} \right] + \left[\begin{array}{c} \hat{d}_{10} \\ \hat{d}_{20} \end{array} \right] \right) + \left[\begin{array}{c} \hat{d}_{12} \\ \hat{d}_{22} \end{array} \right], \\ \left[\begin{array}{c} \hat{d}_{11} \\ \hat{d}_{21} \end{array} \right] &= \left[\begin{array}{c} h_{12} \\ h_{22} \end{array} \right] + B \left[\begin{array}{c} \dot{x} \\ \dot{\theta} \end{array} \right], \end{aligned} \tag{5}$$

$$\begin{aligned} \left[\begin{array}{c} \dot{h}_{13} \\ \dot{h}_{23} \end{array} \right] &= -C\left(-D^{-1}(\theta) \left[\begin{array}{c} -mr\dot{\theta}^2 \sin\theta + kx \\ -\tau \end{array} \right] + \left[\begin{array}{c} \hat{d}_{10} \\ \hat{d}_{20} \end{array} \right] \right), \\ \left[\begin{array}{c} \hat{d}_{12} \\ \hat{d}_{22} \end{array} \right] &= \left[\begin{array}{c} h_{13} \\ h_{23} \end{array} \right] + C \left[\begin{array}{c} \dot{x} \\ \dot{\theta} \end{array} \right], \end{aligned} \tag{6}$$

where

$$A = \begin{bmatrix} a_{11} & a_{12} \\ a_{21} & a_{22} \end{bmatrix}, B = \begin{bmatrix} b_{11} & b_{12} \\ b_{21} & b_{22} \end{bmatrix}, C = \begin{bmatrix} c_{11} & c_{12} \\ c_{21} & c_{22} \end{bmatrix},$$

a_{ij}, b_{ij}, and c_{ij} are constants (i, j =1, 2). In (4)–(6) we set $\hat{d}_{i0}$, $\hat{d}_{i1}$, $\hat{d}_{i2}$ to be the estimated value of the disturbance d_i, $\dot{d}_i$, and $\ddot{d}_i$, respectively $(i = 1, 2)$. We define the estimated error vector to be

$$\begin{gathered} \eta = \begin{bmatrix} \tilde{d}_{10} & \tilde{d}_{20} & \tilde{d}_{11} & \tilde{d}_{21} & \tilde{d}_{12} & \tilde{d}_{22} \end{bmatrix}^T, \\ \tilde{d}_{i0} = d_i - \hat{d}_{i0},\ \tilde{d}_{i1} = \dot{d}_i - \hat{d}_{i1},\ \tilde{d}_{i2} = \ddot{d}_i - \hat{d}_{i2},\ i = 1,\ 2. \end{gathered} \tag{7}$$

Combining (2), (4), (5), and (6) yields

$$\begin{bmatrix} \dot{\hat{d}}_{10} \\ \dot{\hat{d}}_{20} \end{bmatrix} = A \begin{bmatrix} \tilde{d}_{10} \\ \tilde{d}_{20} \end{bmatrix} + \begin{bmatrix} \hat{d}_{11} \\ \hat{d}_{21} \end{bmatrix}, \tag{8}$$

$$\begin{bmatrix} \dot{\hat{d}}_{11} \\ \dot{\hat{d}}_{21} \end{bmatrix} = B \begin{bmatrix} \tilde{d}_{10} \\ \tilde{d}_{20} \end{bmatrix} + \begin{bmatrix} \hat{d}_{12} \\ \hat{d}_{22} \end{bmatrix}, \tag{9}$$

$$\begin{bmatrix} \dot{\hat{d}}_{12} \\ \dot{\hat{d}}_{22} \end{bmatrix} = C \begin{bmatrix} \tilde{d}_{10} \\ \tilde{d}_{20} \end{bmatrix}. \tag{10}$$

From (7)– (9), it is not difficult to obtain the error equation as

$$\begin{gathered} \dot{\eta} = H_1 \eta + E\xi, \\ H_1 = \begin{bmatrix} -A & I_2 & 0 \\ -B & 0 & I_2 \\ -C & 0 & 0 \end{bmatrix},\ E = \begin{bmatrix} 0 \\ 0 \\ I_2 \end{bmatrix},\ \xi = \begin{bmatrix} \dddot{d}_1 & \dddot{d}_2 \end{bmatrix}^T. \end{gathered} \tag{11}$$

Theorem 1. *If the gain matrices A, B, and C in (11) satisfy that H_1 is a Hurwitz matrix, then the estimated disturbance error η is bounded.*

Proof. Since H_1 is a Hurwitz matrix, the matrix equation $P^T H_1 + H_1^T P = -Q$ has only a positive-definite solution P for any positive-definite matrix Q. Choosing a Lyapunov function of (11) to be $V_\eta = \eta^T P \eta$, we have

$$\lambda_{\min}(P)\|\eta\|_2^2 = \lambda_{\min}(P)\eta^T\eta \le V_\eta \le \lambda_{\max}(P)\eta^T\eta = \lambda_{\max}(P)\|\eta\|_2^2 \ .$$

It

$$\frac{V_\eta}{\lambda_{\min}(P)} \ge \|\eta\|_2^2 \ge \frac{V_\eta}{\lambda_{\max}(P)} \ . \tag{12}$$

It follows from (11) that

$$\dot{V}_\eta = \dot{\eta}^T P\eta + \eta^T P\dot{\eta} = -\eta^T Q\eta + 2\eta^T P\xi \le -\lambda_{\min}(Q)\|\eta\|_2^2 + 2\lambda_{\max}(P)\|\eta\|_2\zeta \ . \tag{13}$$

Substituting (12) into (13) yields

$$\dot{V}_\eta \le -\frac{\lambda_{\min}(Q)}{\lambda_{\max}(P)} V_\eta + \frac{2\zeta\lambda_{\max}(P)}{\sqrt{\lambda_{\min}(P)}}\sqrt{V_\eta} \ . \tag{14}$$

Let $\mu = \frac{\lambda_{\min}(Q)}{\lambda_{\max}(P)} V_\eta$, $\upsilon = \frac{2\zeta\lambda_{\max}(P)}{\sqrt{\lambda_{\min}(P)}}$. From (14), we have

$$\dot{\sqrt{V}}_\eta \le -\frac{\mu}{2}\sqrt{V_\eta} + \frac{\upsilon}{2} \ .$$

Solving the equation gives

$$\sqrt{V_\eta} \le \sqrt{V_{\eta 0}} e^{\int_{t_0}^{t} \frac{\mu}{2} d\tau} + \int_{t_0}^{t} e^{\int_{t_0}^{s} \left(-\frac{\mu}{2}\right) d\tau} \frac{\upsilon}{2} ds \le \left(\sqrt{V_{\eta 0}} - \frac{\upsilon}{\mu}\right) e^{-\frac{\mu}{2}(t-t_0)} + \frac{\upsilon}{\mu} \ . \tag{15}$$

From (15), the following inequality holds when $t \to \infty$

$$\sqrt{V_\eta} \le \frac{\upsilon}{\mu} \ . \tag{16}$$

Since $V_\eta \ge \lambda_{\min}(P)\|\eta\|_2^2$, we obtain $\|\eta\|_2 \le \frac{\upsilon}{\mu\sqrt{\lambda_{\min}(P)}}$. The proof is completed. □

4. Design of Robust Stabilization Controller

For the system (1), we construct a coordinate transformation to be

$$\begin{cases} z_1 = x + \frac{mr\sin\theta}{M+m}, \\ z_2 = (M+m)\dot{x} + mr\dot{\theta}\cos\theta, \\ z_3 = \theta, \\ z_4 = \dot{\theta}. \end{cases} \tag{17}$$

The inverse transformation of (17) is

$$\begin{cases} x = z_1 - \frac{mr\sin z_3}{M+m}, \\ \dot{x} = \frac{1}{(M+m)}(z_2 - mrz_4\cos z_3), \\ \theta = z_3, \\ \dot{\theta} = z_4. \end{cases} \tag{18}$$

It is clear that $\left[x, \dot{x}, \theta, \dot{\theta}\right]^T = [0,0,0,0]^T$ and $[z_1, z_2, z_3, z_4]^T = [0,0,0,0]^T$ are equivalent. From (1), we have

$$\begin{cases} \dot{z}_1 = \frac{1}{M+m} z_2, \\ \dot{z}_2 = \Psi(z_1, z_3) + \delta_1^*, \\ \dot{z}_3 = z_4, \\ \dot{z}_4 = \gamma(z_1, z_2, z_3, z_4) + f(z_3)\tau + \delta_2^*, \end{cases} \tag{19}$$

where

$$\Psi(z_1, z_3) = -kz_1 + \frac{kmr}{M+m}\sin z_3 - \alpha z_3, \ \ \delta_1^* = d_1^* + \alpha z_3,$$

$$\gamma(z_1, z_2, z_3, z_4) = \frac{-m^2r^2z_4^2\sin z_3\cos z_3 + kmr[z_1 - (M+m)^{-1}mr\sin z_3]\cos z_3}{\beta(\theta)},$$

$$f(z_3) = \frac{(M+m)}{\beta(\theta)} > 0, \ \ \delta_2^* = \frac{(M+m)d_2^* - mr\cos\theta d_1^*}{\beta(\theta)}, \ \ \beta(\theta) = \det D(\theta).$$

It can be deduced from (3) that

$$\begin{aligned} \delta_1^* &= (M+m)d_1 + mr\cos z_3 d_2 + \alpha z_3 \ , \\ \delta_2^* &= d_2, \\ \dot{\delta}_1^* &= (M+m)\dot{d}_1 + mr\cos z_3\dot{d}_2 + \alpha z_4 - mrz_4\sin z_3 d_2 \ , \\ \ddot{\delta}_1^* &= (M+m)\ddot{d}_1 + mr\cos z_3\ddot{d}_2 + \alpha\dot{z}_4 - 2mrz_4\sin z_3\dot{d}_2 \\ &\quad - mr\dot{z}_4\sin z_3 d_2 - mrz_4^2\cos z_3 d_2 \ . \end{aligned} \tag{20}$$

For the system (19), the main task in this section is to design a controller that guarantees the robust stabilization of the system at the origin. From (20), we choose

$$\begin{aligned}
\hat{\delta}_1^* =&(M+m)\hat{d}_{10} + mr\cos z_3\hat{d}_{20} + \alpha z_3\,,\\
\hat{\delta}_2^* =&\hat{d}_{20},\\
\hat{\delta}_{11}^* =&(M+m)\hat{d}_{11} + mr\cos z_3\hat{d}_{21} + \alpha z_4 - mrz_4\sin z_3\hat{d}_{20}\,,\\
\hat{\delta}_{12}^* =&(M+m)\hat{d}_{12} + mr\cos z_3\hat{d}_{22} - 2mrz_4\sin z_3\hat{d}_{21}\\
&+ \alpha\dot{z}_4 - (mr\dot{z}_4\sin z_3 + mrz_4^2\cos z_3)\hat{d}_{20}\,.
\end{aligned} \tag{21}$$

to be the estimated value of δ_1^*, δ_2^*, $\dot{\delta}_1^*$, and $\ddot{\delta}_1^*$, respectively, and we further obtain

$$\begin{aligned}
\dot{\hat{\delta}}_1^* =&(M+m)\dot{\hat{d}}_{10} + mr\cos z_3\dot{\hat{d}}_{20} + \alpha z_4 - mrz_4\sin z_3\hat{d}_{20}\,,\\
\dot{\hat{\delta}}_{11}^* =&(M+m)\dot{\hat{d}}_{11} + mr\cos z_3\dot{\hat{d}}_{21} + \alpha\dot{z}_4 - mrz_4\sin z_3\hat{d}_{21} - mrz_4\sin z_3\dot{\hat{d}}_{20}\\
&- (mr\dot{z}_4\sin z_3 + mrz_4^2\cos z_3)\hat{d}_{20}\,.
\end{aligned} \tag{22}$$

Define the following variables

$$\begin{cases}
\chi_1 = z_1,\\
\chi_2 = z_2,\\
\chi_3 = \Psi(z_1,z_3) + \hat{\delta}_1^*,\\
\chi_4 = \frac{d\Psi}{dt} + \hat{\delta}_{11}^*.
\end{cases} \tag{23}$$

It follows from (19) and (23) that

$$\begin{cases}
\dot{\chi}_1 = \frac{\chi_2}{M+m},\\
\dot{\chi}_2 = \Psi(z_1,z_3) + \delta_1^*,\\
\dot{\chi}_3 = \frac{d\Psi}{dt} + \dot{\hat{\delta}}_1^*,\\
\dot{\chi}_4 = \frac{d^2\Psi}{dt^2} + \dot{\hat{\delta}}_{11}^*,
\end{cases} \tag{24}$$

where

$$\begin{aligned}
\frac{d\Psi}{dt} &= \frac{\partial\Psi}{\partial z_1}\cdot\frac{z_2}{M+m} + \frac{\partial\Psi}{\partial z_3}\cdot z_4\\
&= -\frac{kz_2}{M+m} + \left[\frac{kmr}{M+m}\cos z_3 - \alpha\right]z_4\,,
\end{aligned}$$

$$\begin{aligned}
\frac{d^2\Psi}{dt^2} =& -\frac{k}{M+m}[\Psi(z_1,z_3)+\delta_1^*] - \frac{kmr}{M+m}\sin z_3\cdot z_4^2\\
&+ \left[\frac{kmr}{M+m}\cos z_3 - \alpha\right]\cdot[\gamma(z) + f(z_3)\tau + \delta_2^*]\\
=& -\frac{k\Psi(z_1,z_3)}{M+m} - \frac{kmr}{M+m}\sin z_3\cdot z_4^2 + \left[\frac{kmr}{M+m}\cos z_3 - \alpha\right]\gamma(z) - \frac{k}{M+m}\delta_1^*\\
&+ \left[\frac{kmr}{M+m}\cos z_3 - \alpha\right]\delta_2^* + \left[\frac{kmr}{M+m}\cos z_3 - \alpha\right]f(z_3)\tau\,.
\end{aligned}$$

We design a sliding mode surface for (24) to be $S = \omega_1\chi_1 + \omega_2\chi_2 + \omega_3\chi_3 + \chi_4$, where $\omega_i > 0$ $(i = 1, 2, 3)$ are constants. Differentiating S along (19) yields

$$\begin{aligned}\dot{S} &= \omega_1\dot{\chi}_1 + \omega_2\dot{\chi}_2 + \omega_3\dot{\chi}_3 + \ddot{\chi}_4\\ &= \omega_1 \cdot \frac{z_2}{M+m} + \omega_2 \cdot \Psi + \omega_3\frac{\partial\Psi}{\partial z_1} \cdot \frac{z_2}{M+m} + \omega_3\frac{\partial\Psi}{\partial z_3}z_4\\ &- \frac{k\Psi(z_1, z_3)}{M+m} - \frac{kmr}{M+m}\sin z_3 \cdot z_4^2 + \left[\frac{kmr}{M+m}\cos z_3 - \alpha\right]\gamma(z) - \frac{k}{M+m}\delta_1^*\\ &+ \left[\frac{kmr}{M+m}\cos z_3 - \alpha\right]\delta_2^* + \left[\frac{kmr}{M+m}\cos z_3 - \alpha\right]f(z_3)\tau\\ &+ \omega_2\delta_1^* + \omega_3\dot{\delta}_1^* + \dot{\delta}_{11}^* .\end{aligned} \tag{25}$$

Based on (25), the equivalent control law is designed to be

$$\begin{aligned}\tau_{eq} = &-\left[\left(\frac{kmr}{M+m}\cos z_3 - \alpha\right)f(z_3)\right]^{-1}\left[\omega_1 \cdot \frac{z_2}{M+m} + \omega_2 \cdot \Psi + \omega_3\frac{\partial\Psi}{\partial z_1} \cdot \frac{z_2}{M+m} + \omega_3\frac{\partial\Psi}{\partial z_3}z_4\right.\\ &- \frac{k\Psi(z_1, z_3)}{M+m} - \frac{kmr}{M+m}\sin z_3 \cdot z_4^2 + \left(\frac{kmr}{M+m}\cos z_3 - \alpha\right)\gamma(z) - \left(\frac{k}{M+m} - \omega_2\right)\hat{\delta}_1^*\\ &\left.+ \left(\frac{kmr}{M+m}\cos z_3 - \alpha\right)\hat{\delta}_2^* + \omega_3\hat{\delta}_{11}^* + \hat{\delta}_{12}^*\right] .\end{aligned} \tag{26}$$

From (20)–(22) we can obtain

$$\begin{aligned}\delta_1^* - \hat{\delta}_1^* &= (M+m)\tilde{d}_{10} + mr\cos z_3\tilde{d}_{20},\\ \dot{\delta}_1^* - \hat{\delta}_{11}^* &= (M+m)\left(\dot{\hat{d}}_1 - \hat{d}_{11}\right) + mr\cos z_3\left(\dot{\hat{d}}_2 - \hat{d}_{21}\right)\\ &= \left[a_{11}(M+m) + a_{21}mr\cos z_3\right]\tilde{d}_{10} + \left[a_{12}(M+m) + a_{22}mr\cos z_3\right]\tilde{d}_{20},\\ \dot{\delta}_{11}^* - \hat{\delta}_{12}^* &= (M+m)\left(\dot{\hat{d}}_{11} - \hat{d}_{12}\right) + mr\cos z_3\left(\dot{\hat{d}}_{21} - \hat{d}_{22}\right) - mrz_4\sin z_3\left(\dot{\hat{d}}_2 - \hat{d}_{21}\right)\\ &= \left[(M+m)b_{11} + mr\cos z_3 b_{21} - a_{21}mrz_4\sin z_3\right]\tilde{d}_{10}\\ &\quad + \left[(M+m)b_{12} + mr\cos z_3 b_{22} - a_{22}mrz_4\sin z_3\right]\tilde{d}_{20},\\ \delta_2^* - \hat{\delta}_2^* &= \tilde{d}_{20} .\end{aligned} \tag{27}$$

Substituting (26) into (25) yields

$$\begin{aligned}\dot{S} = &\left\{\left[-\frac{k}{M+m} + \omega_2\right](M+m) + \omega_3[a_{11}(M+m) + a_{21}mr\cos z_3] +\right.\\ &\left.\left[(M+m)b_{11} + b_{21}mr\cos z_3 - a_{21}mrz_4\sin z_3\right]\right\}\tilde{d}_{10}\\ &+ \left\{\left[-\frac{k}{M+m} + \omega_2\right]mr\cos z_3 + \omega_3[a_{12}(M+m) + a_{22}mr\cos z_3] +\right.\\ &\left.(M+m)b_{12} + b_{22}mr\cos z_3 - a_{22}mrz_4\sin z_3 + \left(\frac{kmr}{M+m}\cos z_3 - \alpha\right)\right\}\tilde{d}_{20}\\ = &Y_1\tilde{d}_{10} + Y_2\tilde{d}_{20} ,\end{aligned} \tag{28}$$

where

$$Y_1 = -k + (M+m)[\omega_2 + \omega_3 a_{11} + b_{11}] + [a_{21}\omega_3 + b_{21}]mr\cos z_3 - a_{21}mrz_4 \sin z_3\,,$$

$$Y_2 = -\alpha + (M+m)[a_{12}\omega_3 + b_{12}] + [\omega_2 + a_{22}\omega_3 + b_{22}]mr\cos z_3 - a_{22}mrz_4 \sin z_3.$$

From (26) and (28), we design the controller τ for (24) as

$$\tau = \tau_{eq} + \tau_1, \tag{29}$$

where

$$\tau_1 = -\left[\left(\frac{kmr}{M+m}\cos z_3 - \alpha\right) f(z_3)\right]^{-1}\left[-|Y_1|\bar{d}_{10} - |Y_2|\bar{d}_{20} - \rho\,\mathrm{sgn}(S) - \varphi S^2\,\mathrm{sgn}(S)\right], \tag{30}$$

where $|\tilde{d}_{10}| \le \bar{d}_{10}$, $|\tilde{d}_{20}| \le \bar{d}_{20}$, φ, and ρ are positive constants. A Lyapunov function for (24) is selected to be $V = \frac{1}{2}S^2$. It follows from (25), (28)–(30)that

$$\begin{aligned}\dot{V} =& S\dot{S} = S\left[Y_1\tilde{d}_{10} + Y_2\tilde{d}_{20} - |Y_1|\bar{d}_{10} - |Y_2|\bar{d}_{20} - \rho\,\mathrm{sgn}(S) - \varphi S^2\,\mathrm{sgn}(S)\right]\\ \le& S\left[-\rho\,\mathrm{sgn}(S) - \varphi S^2\,\mathrm{sgn}(S)\right] = -\rho|S| - \varphi S^2|S|\\ =& -\rho|S| - \varphi|S|^3 = -\rho\sqrt{2}V^{\frac{1}{2}} - \varphi\sqrt{2^3}V^{\frac{3}{2}} \le 0.\end{aligned} \tag{31}$$

According to Lemma 3 in [24], S converges to 0 in a fixed time when (31) is satisfied, and the settling time t_f satisfies that

$$t_f \le \frac{1}{\varphi\sqrt{2^3}(\frac{3}{2}-1)} + \frac{1}{\rho\sqrt{2}(1-\frac{1}{2})} = \frac{1}{\varphi\sqrt{2}} + \frac{\sqrt{2}}{\rho}\,.$$

From the above statements, we know that the system (24) can reach the sliding surface $S = 0$ by the control input τ in (29). When $S = 0$, it follows from (24) that

$$\begin{aligned}&\dot{\chi} = H_2\chi + \Delta,\\ &\begin{cases}\chi = \begin{bmatrix}\chi_1 & \chi_2 & \chi_3\end{bmatrix}^T, \Delta = \begin{bmatrix}0 & \delta_1^* - \delta_1^* & \dot{\delta}_1^* - \delta_{11}^*\end{bmatrix}^T,\\ H_2 = \begin{bmatrix}0 & \frac{1}{M+m} & 0\\ 0 & 0 & 1\\ -\omega_1 & -\omega_2 & -\omega_3\end{bmatrix}, \chi_4 = -\omega_1\chi_1 - \omega_2\chi_2 - \omega_1\chi_3.\end{cases}\end{aligned} \tag{32}$$

Note that $\delta_1^* - \hat{\delta}_1^*$ and $\dot{\delta}_1^* - \hat{\dot{\delta}}_{11}^*$ are bounded from (27). It is assumed that the matrix H_2 in (32) is a Hurwitz matrix for appropriate parameters ω_1, ω_2, and ω_3. Following the same proof of Theorem 1 gives that χ_1, χ_2, χ_3, and χ_4 are ultimately uniformly bounded around a small ball of the origin. As a result, the robust stabilization control of (19) at the origin is achieved.

5. Numerical Examples

In this section, two numerical examples are presented to verify the effectiveness of our developed control strategy.

The parameters of the TORA system were selected to be [17]:

$$M = 1\ \mathrm{kg},\ \mathrm{m} = 0.4\ \mathrm{kg},\ \mathrm{r} = 0.025\ \mathrm{kg}\cdot\mathrm{m}^2,\ \mathrm{k} = 15\ \mathrm{N/m}. \tag{33}$$

The initial state of the TORA system was chosen to be

$$\left[\ x,\ \dot{x},\ \theta,\ \dot{\theta}\right]^{\mathrm{T}} = \left[\ 0.5,\ 0.6,\ 0.6,\ 0.5\right]^{\mathrm{T}}. \tag{34}$$

Moreover, the gain matrices in (4), (5), and (6) were selected as

$$A = \begin{bmatrix} a_{11} & a_{12} \\ a_{21} & a_{22} \end{bmatrix} = 10I_2,\ B = \begin{bmatrix} b_{11} & b_{12} \\ b_{21} & b_{22} \end{bmatrix} = 90I_2,\ C = \begin{bmatrix} c_{11} & c_{12} \\ c_{21} & c_{22} \end{bmatrix} = 295I_2. \tag{35}$$

It is easy to verify that the matrix H_1 in (11) is a Hurwitz matrix with eigenvalues $\nu_{1,2,3,4} = -2.73 \pm 7.59j$, $\nu_{5,6} = -4.52$. The parameters in the controllers (26) and (30) were designed to be

$$\omega_1 = 2, \omega_2 = 1000, \omega_3 = 200, \sigma = 100, \rho = 100\ . \tag{36}$$

Suppose the diaturbances are

$$d_1^* = 0.1\sin t - 10\theta,\ d_2^* = 0.1\sin t + 0.05 + 0.1\dot{\theta}. \tag{37}$$

Figure 2 shows the simulation results of the disturbance d_i and its estimated value $\hat{d}_{i0}(i = 1, 2)$. Note that the disturbance observer (4)–(6) has good estimation accuracy for the disturbances. Under the operation of the robust controller (29), the time responses of the TORA system are shown in Figure 3. It is clear that the controller (29) can overcome the influence of disturbances, and the TORA system achieves robust stabilizing control objective at the origin position better. These show the effectiveness of our developed theoretical analysis results.

In order to further verify the advantage of our developed method, we carried out a comparative simulation experiment. The same initial value and the disturbance of the system were chosen as in Ref. [21]

$$\left[\ x,\ \dot{x},\ \theta,\ \dot{\theta}\right]^{\mathrm{T}} = \left[\ -0.5,\ 0,\ 0.5,\ 0\right]^{\mathrm{T}}, d_2^* = \frac{10\sin t}{10 + 0.5t^2}. \tag{38}$$

The simulation results under the above conditions are shown in Figure 4. It is clear that our method can still achieve the robust stabilization of the TORA. The settling time is less than 4 s. In contrast, the settling time in [21] is about 25 s. This shows the advantage of the presented method in this paper. In addition, the method presented in [21] is only applicable to the system with matched disturbances. In comparison, our presented method is applicable to the system with both matched and/or mismatched disturbances. Thus, our method has a wider application range than that in Ref. [21].

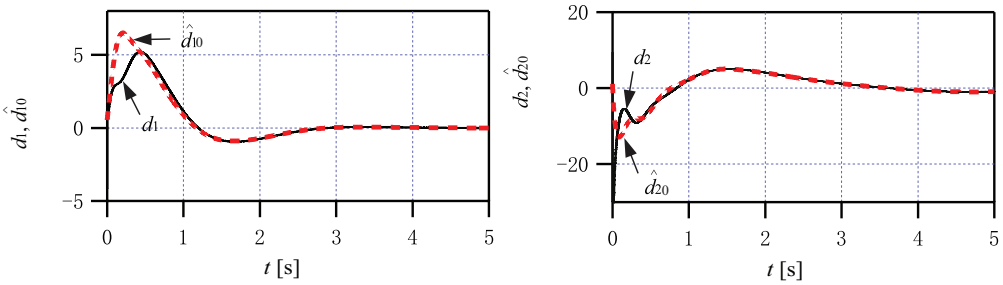

Figure 2. Actual value and observed values of the disturbances d_1 and d_2 in (37).

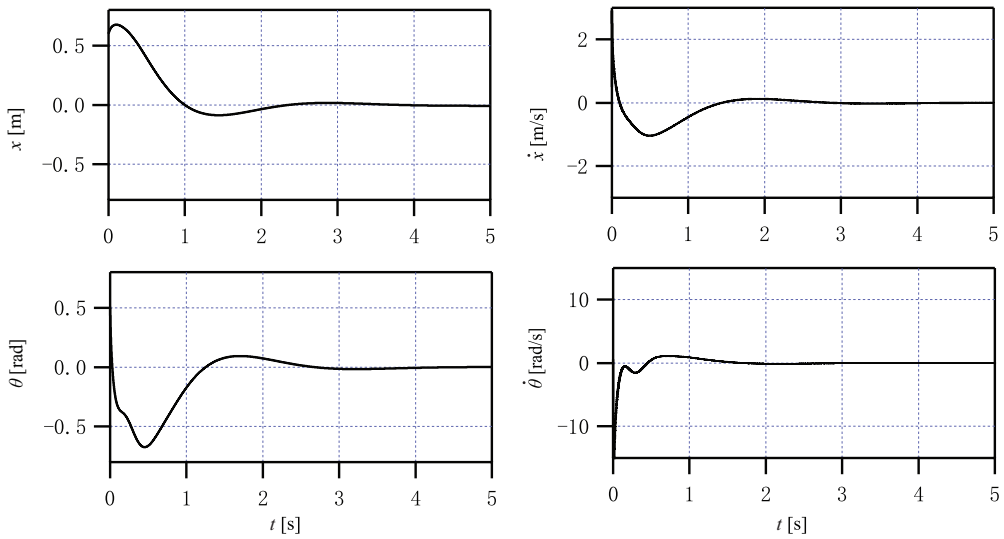

Figure 3. Time responses of the TORA system by the robust controller (29) with (34) and (37).

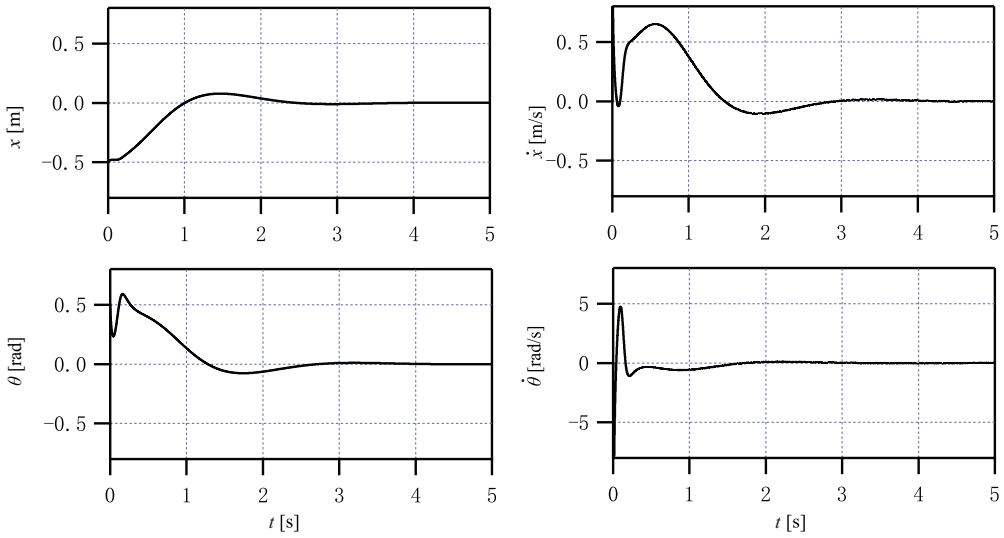

Figure 4. Time responses of the TORA system by the robust controller (29) with (38).

6. Conclusions

This paper discussed the robust stabilization control of an underactuated TORA system with multiple external disturbances. First, a nonlinear disturbance observer was constructed to quickly estimate the external disturbances. Then, the coordinate transformation and fixed-time sliding mode control method were used to design a robust controller, and the simulation results demonstrated the validity of our presented theoretical analysis results. In the future, we will further study other design methods for robust stabilzation controllers for the TORA system on the basis of research results in this paper.

Author Contributions: Methodology, Q.F. and A.Z.; formal analysis, X.Z., G.P. and Z.L.; writing—original draft, Q.F.; writing—review and editing, A.Z. All authors have read and agreed to the published version of the manuscript.

Funding: This work was supported in part by the Natural Science Foundation Program of Shandong Province under Grant no. ZR2019YQ28, the Development Plan of Youth Innovation Team of University in Shandong Province under Grant no. 2019KJN007, and the National Natural Science Foundation of China under Grant Nos. 61773193, 62103177 and 61903171.

Institutional Review Board Statement: Not applicable.

Informed Consent Statement: Not applicable.

Data Availability Statement: The readers can access the data reported in this paper from the corresponding author.

Conflicts of Interest: The authors declare no conflict of interest.

References

1. Rand, R.H.; Kinsey, R.J.; Mingori, D.L. Dynamics of spinup through resonance. *Int. J. Nonlin. Mech.* **1992**, *27*, 489–502. [CrossRef]
2. Avis, J.M.; Nersesov, S.G.; Nathan, R.; Ashrafiuon, H.; Muske, K.R. A comparison study of nonlinear control techniques for the rtac system. *Nolinear Anal. -Real.* **2010**, *11*, 2647–2658. [CrossRef]
3. Sa' Id, W.; Al-Samarraie, S.; Mshari, M. Simple flatness condition for 2-DOF underactuated mechanical systems with application to controller design. *Math. Model. Eng. Probl.* **2020**, *7*, 119–126. [CrossRef]
4. Zhao, G.; Li, H.; Song, Z. Adaptive dynamic fuzzy neural network-based decoupled sliding-mode controller with hybrid sliding surfaces. *Int. J. Autom. Control* **2013**, *7*, 183–201. [CrossRef]
5. Tadmor, G. Dissipative design, lossless dynamics, and the nonlinear TORA benchmark example. *IEEE Trans. Control. Syst. Technol.* **2001**, *9*, 391–398. [CrossRef]
6. Jankovic, M.; Fontaine, D.; Kokotovic, P.V. TORA example: Cascade and passivity-based control designs. *IEEE Trans. Control. Syst. Technol.* **1996**, *4*, 292–297. [CrossRef]
7. Liu, Y.; Yu, H. A survey of underactuated mechanical systems. *IET Control. Theory Appl.* **2013**, *7*, 921–935. [CrossRef]
8. Gao, B.; Xu, J.; Zhao, J.; Huang, X. Stabilizing control of an underactuated 2-dimensional TORA with only rotor angle measurement. *Asian J. Control.* **2013**, *15*, 1477–1488. [CrossRef]
9. Gutiérrez-Oribio, D.; Mercado-Uribe, J.A.; Moreno, J.A.; Fridman, L. Robust global stabilization of a class of underactuated mechanical systems of two degrees of freedom. *Int. J. Robust. Nonlin.* **2021**, *31*, 3908–3928. [CrossRef]
10. Sun, N.; Wu, Y.; Fang, Y.; Chen, H.; Lu, B. Nonlinear continuous global stabilization control for underactuated RTAC systems: Design, analysis, and experimentation. *IEEE-Asme T. Mech.* **2016**, *22*, 1104–1115. [CrossRef]
11. Feng, Q.; Zhang, A.; Li, N. Design of stabilizing controllers for underactuated TORA system. In Proceedings of the 2021 China Automation Congress (CAC), Beijing, China, 22–24 October 2021; pp. 3323–3327.
12. Liu, D.; Guo, W. Nonlinear backstepping design for the underactuated TORA system. *J. Vibroeng.* **2014**, *16*, 552–559.
13. Alleyne, A. Physical insights on passivity-based TORA control designs. *IEEE Trans. Control. Syst. Technol.* **1998**, *6*, 436–439. [CrossRef]
14. Xu, R.; Özgüner, Ü. Sliding mode control of a class of underactuated systems. *Automatica* **2008**, *44*, 233–241. [CrossRef]
15. Wu, T.; Gui, W.; Hu, D.; Du, C. Adaptive fuzzy sliding mode control for translational oscillator with rotating actuator: A fuzzy model. *IEEE Access* **2018**, *6*, 55861–55869. [CrossRef]
16. Gao, B.; Ye, F. Fuzzy Lyapunov synthesis control of an underactuated 2D TORA system. *J. Intell. Fuzzy Syst.* **2015**, *28*, 581–589. [CrossRef]
17. She, J.; Zhang, A.; Lai, X.; Wu, M. Global stabilization of 2−DOF underactuated mechanical systems an equivalent-input-disturbance approach. *Nonlinear Dynam.* **2012**, *69*, 495–509. [CrossRef]
18. Sun, N.; Wu, Y.; Fang, Y.; Chen, H. Nonlinear stabilization control of multipleRTAC systems subject to amplitude-restricted actuating torques using only angular position feedback. *IEEE Trans. Ind. Electron.* **2017**, *64*, 3084–3094. [CrossRef]
19. Wu, Y.; Sun, N. ; Fang, Y.; Liang, D. An increased nonlinear coupling motion controller for underactuated multi—TORA systems: Theoretical design and hardware experimentation. *IEEE Trans. Syst. Man Cybern. Part B* **2017**, *49*, 1186–1193. [CrossRef]
20. Tavakoli, M.; Taghirad, H.D.; Abrishamchian, M. Identification and robust $H\infty$control of the rotational/translational actuator system. *Int. J. Control Autom.* **2005**, *3*, 387–396.
21. Wu, X.; Zhao, Y.; Xu, K. Nonlinear disturbance observer based sliding mode control for a benchmark system with uncertain disturbances. *ISA Trans.* **2020**, *110*, 63–70. [CrossRef]
22. Huang, J.; Ri, S.; Fukuda, T.; Wang, Y. A disturbance observer based sliding mode control for a class of underactuated robotic system with mismatched uncertainties. *IEEE Trans. Autom. Control* **2019**, *64*, 2480–2487. [CrossRef]
23. Li, S.; Sun, H.; Yang, J.; Yu, X. Continuous finite-time output regulation for disturbed systems under mismatching condition. *IEEE Trans. Autom. Control* **2015**, *60*, 277–282. [CrossRef]
24. Parsegov, S.E.; Polyakov, A.E.; Shcherbakov, P.S. Fixed-time consensus algorithm for multi-agent systems with integrator dynamics. *IFAC J. Syst. Control* **2013**, *46*, 110–115. [CrossRef]